Metal Insertion Route of the Ni + CO_2 → NiO + CO Reaction

Yacine Hannachi* and Joëlle Mascetti

Laboratoire de Physico-Chimie Moléculaire, (CNRS UMR 5803), Université Bordeaux I, 33405 Talence Cedex, France

András Stirling† and Imre Pápai*

Institute of Chemistry, Theoretical Chemistry Department, Chemical Research Center of HAS, Pusztaszeri út 59-67, H-1025 Budapest, Hungary

Received: April 27, 2003; In Final Form: June 10, 2003

The gas-phase reaction of the nickel atom with CO_2 molecule is investigated at the B3LYP and CCSD(T) levels of theory. The insertion−elimination route to NiO ($^3\Sigma^-$) + CO ($^1\Sigma^+$) is found to be the most favorable mechanism. The insertion product on the $^3A''$ surface is calculated to be about 15 kcal/mol higher in energy than the reactants. The insertion reaction is direct and needs to overcome an energy barrier of 34.6 kcal/mol. A second path, on the $^3A'$ surface, is similar but the insertion product is less stable with respect to the corresponding $^3A''$ species and the transition state is higher in energy. The $^3A''$ insertion product can dissociate to NiO ($^3\Sigma^-$) + CO ($^1\Sigma^+$) without exit barrier. This reaction is endothermic by 22 kcal/mol. The $^3A'$ insertion product can also dissociate without exit barrier but leads to an excited state of nickel oxide (A $^3\Pi$). The Ni + CO_2 → NiO + CO reaction is found to be endothermic by 37.4 kcal/mol in good agreement with experiment (36.6 kcal/mol).

1. Introduction

The catalytic activation of carbon dioxide, this abundant but thermodynamically stable and inert compound, has long been of challenge in synthetic chemistry.[1−9] The fixation of CO_2 by metallic centers is thought to be a key step in these processes, therefore, several experimental and theoretical studies have focused on the interaction of CO_2 and transition metal atoms[10−43] trying to explore the thermochemistry and kinetics of these reactions. One of the most extensively investigated systems is Ni + CO_2,[19,23,36−39] which is not surprising given that nickel catalysts have been shown to be particularly promising in this field too.

The first matrix isolation experiments carried out on Ni + CO_2[19] revealed that no reaction occurs between thermally evaporated Ni atoms and CO_2 in argon-diluted matrixes; however, clear evidence for the existence of 1:1 type Ni(CO_2) complexes has been found in a neat CO_2 matrix. On the basis of further matrix isolation FTIR studies using isotopically labeled species and also the results of density functional calculations,[36] these complexes were identified as side-on (η^2_{CO}) coordinated Ni(CO_2) species. The calculations predicted the singlet $^1A'$ state of the η^2_{CO}-Ni(CO_2) complex to be the most stable form among the possible 1:1 coordination modes, but the triplet state of this complex was also found to correspond to a minimum on a relevant potential energy surface lying about 15 kcal/mol higher in energy than the $^1A'$ ground state.

Laser ablated Ni atoms, owing to their excess kinetic energy, were shown to cleave the CO_2 molecule, resulting in NiO−carbonyl species.[23] The ONiCO complex was assumed to be formed via the insertion of the metal atom into a C−O bond of CO_2, a process demonstrated to occur spontaneously between early transition metal atoms and CO_2.[33−35,40−43] Related DFT calculations[23] indicated that $^3A''$ is the ground state of ONiCO, which could also be produced via the association of NiO and CO induced by annealing the matrix sample after photolytic excitation.[23]

The only theoretical approach aiming at describing the mechanism of the entire Ni + CO_2 → NiO + CO oxygen abstraction reaction was presented by Mebel and Hwang,[39] who proposed that the lowest energy route for this reaction corresponds to the formation of a cyclic η^2_{OO}-Ni(CO_2) ($^3B_1$) intermediate, which undergoes a Ni−O bond cleavage to form the linear CONiO complex prior to NiO + CO dissociation. Interestingly, the authors did not consider the metal insertion pathway, although the laser ablation matrix isolation experiments[23] clearly demonstrated the intermediacy of the ONiCO insertion species.

In the present work, we intended to explore the insertion route on the Ni + CO_2 → NiO + CO potential energy surface and conclude about the mechanism of this reaction.

2. Computational Details

Because here we are mostly concerned with the reactivity of the ground state Ni atom, we investigate the lowest lying triplet $^3A''$ and $^3A'$ potential energy surfaces.[44] The stationary points on these surfaces were located using B3LYP density functional calculations[45−47] with a basis set that includes the (14,9,5)/[8,5,3] all-electron Ni basis set of Schäfer, Horn, and Ahlrichs[48] supplemented with two polarization p functions[49] and a diffuse d function,[50] and the 6-311+G(2d) basis set for carbon and oxygen.[51] For simplicity, this basis set will be referred to as 6-311+G(2d)′ throughout the paper. Vibrational frequency

* Corresponding authors. E-mail: Y.H., y.hannachi@lpcm.u-bordeaux1.fr; I.P., papai@chemres.hu.

† Present address: Centro Svizzero di Calcolo Scientifico (CSCS), Manno and ETH Zurich, Switzerland.

10.1021/jp0351324 CCC: $25.00
Published on Web 08/01/2003

calculations were performed at this level to verify the identity of the stationary points and also to estimate the zero-point energies (ZPE). For each transition state, intrinsic reaction coordinate (IRC) calculations[52] were carried out in both directions (with a step size of 0.1 amu$^{1/2}$ bohr) to connect these saddle-points to the respective minima.

The geometries of the located stationary points were reoptimized at the B3LYP/6-311+G(3df)′ level, where 6-311+G(3df)′ denotes the standard 6-311+G(3df) basis set without the Ni g polarization functions.[53] As a next step, single-point CCSD(T)/6-311+G(3df)′ energy calculations were carried out at the B3LYP/6-311+G(3df)′ stationary points. The correlation treatment in the coupled cluster calculations[54,55] involved all valence electrons. The stability of the single-determinant wave function was checked for each stationary point. All energies discussed in the paper are those obtained at the CCSD(T)/6-311+G(3df)′ level unless otherwise noted in the text. As seen later, the relative energies obtained at the B3LYP are very similar to those obtained at the CCSD(T) level. This is, however, not a general rule and this agreement is not obtained for other similar systems (see, for example, ref 43)

The ground state of the nickel atom is $^3F_4$ ($4s^23d^8$ electronic configuration), but the $^3D_3$ ($4s^13d^9$ electronic configuration) state is only 0.59 kcal/mol higher in energy.[56] However, when the energy levels are averaged over all orbit−spin components the ^3D state is 0.72 kcal/mol lower in energy.[56] The CCSD(T) value (1.1 kcal/mol) reproduces fairly well this energy gap, whereas B3LYP overestimates the experimental value by about 9 kcal/mol. In the following, the relative energies of the intermediates and products are then given with respect to that calculated for Ni (^3D, $4s^13d^9$) + CO_2 ($^1\Sigma^+_g$).

For selected structures, atomic populations (atomic charges, electron configuration, etc) are given. These data were derived from natural bond orbital (NBO) analysis[57] carried out for the relevant structures at the B3LYP/6-311+G(2d)′ level.

All calculations in the present study were performed with the Gaussian98 program.[58]

3. Results and Discussion

(a) Metal Insertion Route. The insertion route involves the cleavage of one of the C−O bonds and the Ni−C and Ni−O bond formations in a concerted way. The optimized structures of the stationary points located on the $^3A''$ and $^3A'$ potential surfaces corresponding to the insertion pathway are shown in Figure 1.[59] The relative stabilities of these species calculated at various levels of theory are listed in Table 1.

The $^3A''$ and $^3A'$ states of the ONiCO insertion product are calculated to be quite close in energy, but all methods predict the ONiCO ($^3A''$) species to be about 2 kcal/mol more stable than ONiCO ($^3A'$). The ONiCO ($^3A''$) complex has a bent equilibrium structure and correlates with the NiO ($^3\Sigma^-$) + CO ($^1\Sigma^+$) dissociation asymptote, because the singly occupied molecular orbitals (20a′ and 6a") in ONiCO ($^3A''$) are characterized as mostly π^* NiO orbitals, which corresponds to its $^3\Sigma^-$ ($\delta^4\sigma^2\pi^2$) ground state. On the other hand, the insertion product formed on the $^3A'$ surface is linear and it dissociates into NiO ($^3\Pi$) + CO ($^1\Sigma^+$), where the $^3\Pi$ state of NiO is an excited state arising from the $\delta^4\sigma^1\pi^3$ electron configuration. On the basis of the experimental Ni−O and OC−O bond dissociation energies (D_o(Ni−O) = 89.1 ± 0.7 kcal/mol,[60] D_o(OC−O) = 125.7 kcal/mol[61]), and on the measured NiO $A^3\Pi-X^3\Sigma^-$ electronic transition (4330 cm^{-1} or 12.4 kcal/mol[62]), the NiO ($^3\Sigma^-$) + CO and NiO ($^3\Pi$) + CO dissociation limits lie 36.6 and 49.0 kcal/mol above the Ni + CO_2 reactants. These experimental values

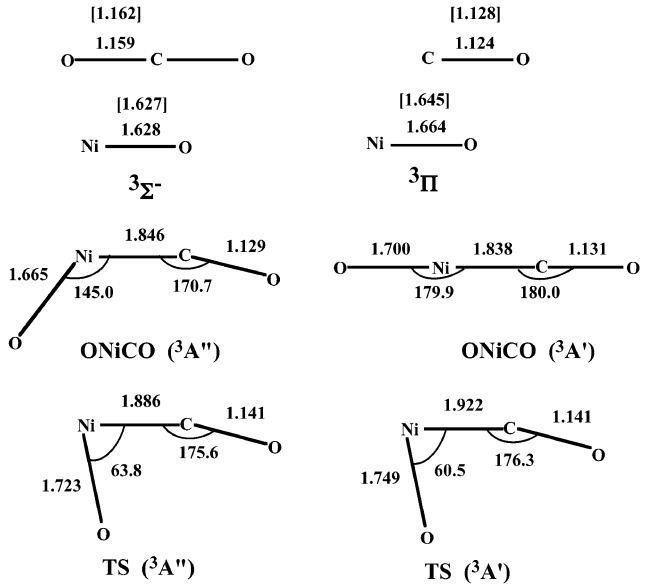

Figure 1. Geometrical parameters of minima and transition states optimized at the B3LYP/6-311+G(3df)′ level (distances in ångstroms, angles in degrees). Experimental data for CO_2,[67] CO,[68] and NiO[69,62] are given in brackets.

TABLE 1: Calculated Relative Energies (kcal/mol, with Respect to Ni (s^1d^9) + CO_2) on the Insertion Pathway[a]

	A	B	C	exp
	$^3A''$ Surface			
ONiCO ($^3A''$)	15.8	17.0	15.4	
TS ($^3A''$)	38.4	39.3	34.6	
NiO ($^3\Sigma^-$) + CO ($^1\Sigma^+$)	44.5	45.6	37.4	36.6[b]
	$^3A'$ Surface			
ONiCO ($^3A'$)	17.5	18.6	17.4	
TS ($^3A'$)	45.6	46.2	45.0	
NiO ($^3\Pi$) + CO ($^1\Sigma^+$)	52.8	53.7	51.7	49.0[c]

[a] Notation used to define the level of theory: A = B3LYP/6-311+G(2d)′, B = B3LYP/6-311+G(3df)′, C = CCSD(T)/6-311+G(3df)′//B3LYP/6-311+G(3df)′. [b] Based on the experimental Ni−O and OC−O bond dissociation energies (D_o(Ni−O) = 89.1 ± 0.7 kcal/mol,[60] D_o(OC−O) = 125.7 kcal/mol[61]). [c] Based on the measured NiO $A^3\Pi-X^3\Sigma^-$ electronic transition (4330 cm^{-1} or 12.4 kcal/mol[62]).

are quite accurately reproduced at the CCSD(T)/6-311+G(3df)′ level, but they are slightly overestimated in the B3LYP calculations (see Table 1).

We attribute the linearity of the $^3A'$ product to the reduced σ-repulsion between the fragments, as the 4σ orbital of the NiO unit is singly occupied in the linear complex and doubly occupied in the bent structure. In addition, the enhanced overlap between the π^* CO orbital and the NiO π orbitals also stabilizes the linear structure. Comparison of the Ni−C bond lengths (1.838 vs 1.846 Å, for the linear and bent complexes, respectively) emphasizes the reduced σ-repulsion, whereas the slightly lengthened CO bond in the linear complex as compared to the bent structure indicates the more optimal π overlap, which destabilizes the C−O interaction.

Similar to our previous studies,[40,43] we constructed potential energy curves as a function of the cleaved C−O bond by constrained geometry optimizations starting from the ONiCO ($^3A''$) and ONiCO ($^3A'$) structures and reducing gradually the C−O bond distance (see Figure 2). The highest energy points on these curves were then used as initial structures for transition state search calculations. The located transition states (TS ($^3A''$) and TS ($^3A'$)) are found to be 34.6 ($^3A''$) and 45.0 ($^3A'$) kcal/mol above the Ni (s^1d^9) + CO_2 reference level, indicating that

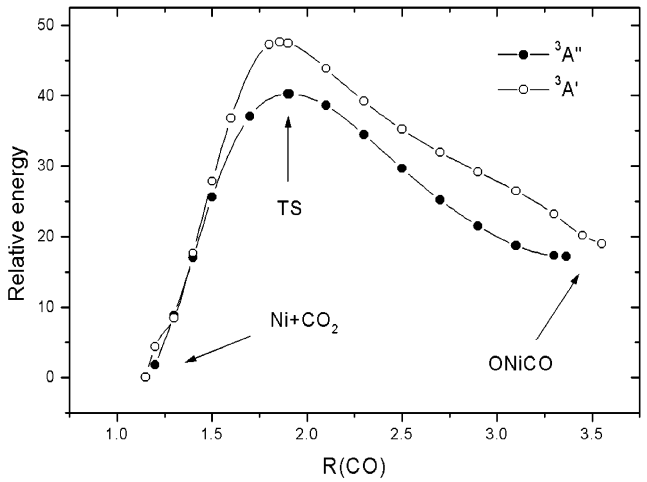

Figure 2. ^{3}A″ and ^{3}A′ potential energy curves derived for the metal insertion route. Relative energy in kcal/mol, *R*(CO) in Å.

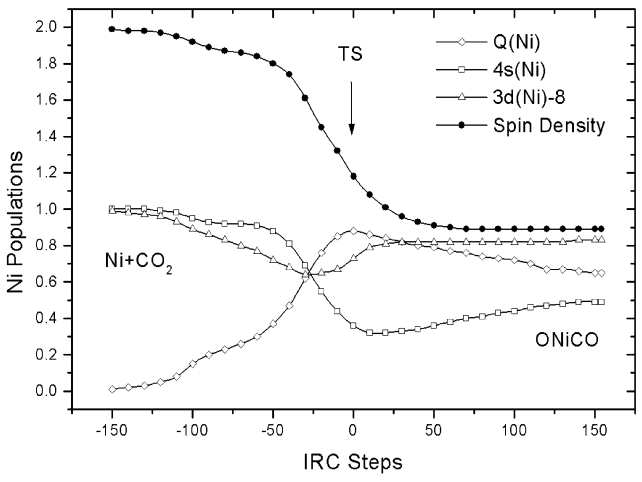

Figure 3. Ni atomic populations along the ^{3}A″ insertion path.

the insertion process requires a fair amount of activation energy, and also that the barrier to metal insertion is about 10 kcal/mol lower on the ^{3}A″ surface.

The constrained geometry optimization procedure, however, did not show a minimum for the η^2_{CO}-Ni(CO_2) structure on the ^{3}A″ and ^{3}A′ potential energy curves, because both states dissociated into Ni (s^1d^9) + CO_2 when the region around R_{C-O} = 1.2 Å was approached. The IRC calculations carried out from the TS (^{3}A″) and TS (^{3}A′) transition structures confirmed that these transition states connect directly both states of ONiCO with the Ni (s^1d^9) + CO_2 reactants. These findings contradict with previous theoretical studies,[23,36] which identified the triplet state of the η^2_{CO}-Ni(CO_2) complex as a minimum. The likely reason for this contradiction is that the calculations predicting the existence of an η^2_{CO} minimum on the triplet surface were all performed with the GGA type BP86 functional,[63,64] which tends to overestimate the strength of metal−ligand interactions, as shown below. Our CCSD(T)/6-311+G(3df)′ calculations carried out for the η^2_{CO}-Ni(CO_2) (^{3}A″) structure optimized at the BP86/6-311+G(3df)′ level indicate a repulsive Ni−CO_2 interaction (ΔE = +6.3 kcal/mol), whereas BP86/6-311+G-(3df)′ gives an attractive interaction (ΔE = −3.6 kcal/mol). In addition, the ONiCO (^{3}A″) species is predicted to be 6.6 kcal/mol lower in energy at the BP86/6-311+G(3df)′ level than the reactants, in contradiction with CCSD(T) results. This provides further support for a direct Ni (s^1d^9) + CO_2 → ONiCO insertion process.

In accord with the Hammond postulate,[65] the transition state of this endothermic insertion reaction involves large structural changes and significant electronic reorganizations. To understand the electronic details of the mechanism and to rationalize these structural changes along the reaction path, we have to analyze the orbital interactions of the reactants that are responsible for the C−O bond breaking and Ni−O bond formation. To this end, we present Figure 3 displaying the variation of the Ni electronic populations as the reaction proceeds along the intrinsic reaction coordinate. The entrance channel of the insertion process can be characterized by a charge transfer from the metal atom toward the CO_2 molecule. Both the 4s and the 3d orbitals participate in the charge donation by overlapping with the in-plane π^* orbital of CO_2. Due to these interactions, we observe the following features at the initial phase of the reaction: The C−O bonds start to weaken and lengthen because of the antibonding character for these bonds. Also, the CO_2 molecule begins to bend as the negatively charged CO_2 stabilizes in a bent structure. In fact, the reaction coordinate is composed to a large extent of the OCO bending, which underlines the importance of the charge transfer. The other two important components of the reaction coordinate are the C−O elongation and the bond formation between the Ni atom and the C and O atoms of the cleaved bond. Clearly, a considerable amount of charge is transferred as the transition state is approached. Figure 3 also shows that the main sources of the donated electrons are the unpaired orbitals of the Ni atom, because the spin density on the Ni atom decreases gradually along the insertion route. The positive charge of Ni is maximized around the transition state and then stabilizes at a somewhat lower value as the product is formed. This implies back-donation from the CO fragment at the later stages of the reaction. Indeed, we notice that in the product channel, during the formation of the NiO and CO units, both the 4s and 3d populations increase slightly. Overall, the Ni electron configuration changed from $4s^13d^9$ to $4s^{0.39}3d^{8.77}$. In general, the insertion mechanism features that the oxygen abstraction and metal insertion take place simultaneously with the electron transfer. Recently, this mechanism has also been proposed for the reactions of NO_2 and N_2O molecules with 3d transition metal atoms.[66]

(b) Alternative Reaction Channels. To compare the energetics of the above insertion process with that of the mechanism investigated by Mebel and Hwang,[39] we considered the η^2_{OO} species and related dissociation channels as well (see Figure 4 and Table 2). We found that the lowest energy structure for the η^2_{OO} coordination mode corresponds to the $^3B_2$ state lying 14.3 kcal/mol above the reactants. We have also located a minimum for the $^3B_1$ state with a structure very similar to that reported by Mebel and Hwang, but our calculations showed that this structure is much less stable than predicted before (34.4 kcal/mol above Ni + CO_2). Moreover, there are further indications that the formation of the $^3B_1$ species is quite unlikely. For instance, calculations to test the stability of the B3LYP/6-311+G(2d)′ and B3LYP/6-311+G(3df)′ single determinants for the geometry presented in Figure 4 found a lower $^3B_1$ solution; however, the geometry optimization for the new solution led to the Ni + CO_2 dissociation. Furthermore, an optimization from a slightly distorted C_{2v} structure of the original $^3B_1$ state converged within a few steps to the $^3B_2$ minimum.

The η^2_{OO}-Ni(CO_2) ($^3B_2$) complex can easily dissociate into Ni + CO_2 as well, because the related transition state (TS′ (^{3}A′)) represents a barrier of only 3 kcal/mol to the separated reactants. To map a route toward the NiO + CO products, we performed constrained geometry optimizations with fixed C−O bond

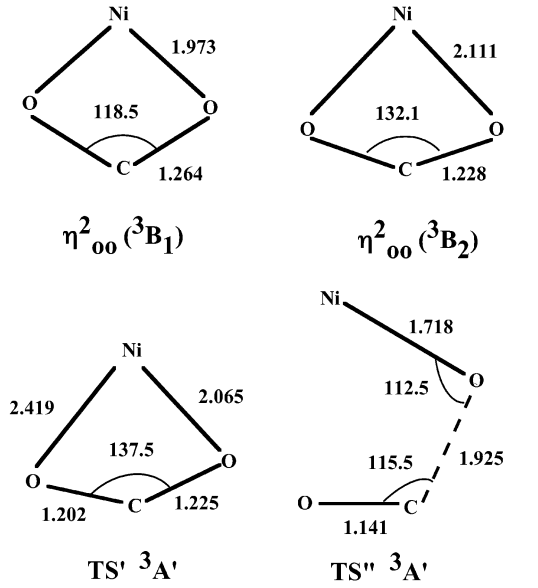

Figure 4. Geometrical parameters of the cyclic species and the related transition states optimized at the B3LYP/6-311+G(3df′ level (distances in ångstroms, angles in degrees).

TABLE 2: Calculated Relative Energies (kcal/mol, with respect to Ni (s^1d^9) + CO_2) Concerning the Cyclic Ni(CO_2) Species[a]

	A	B	C
η^2_{OO}-Ni(CO_2) ($^3B_2$)	16.5	16.9	14.3
TS′ (^{3}A′)	16.7	17.0	17.2
TS" (^{3}A′)	58.0	59.0	59.9
η^2_{OO}-Ni(CO_2) ($^3B_1$)[b]	40.8	41.0	34.4

[a] Notation used to define the level of theory: A = B3LYP/6-311+G(2d)′, B = B3LYP/6-311+G(3df)′, C = CCSD(T)/6-311+G-(3df)′//B3LYP/6-311+G(3df)′. [b] Unstable solution.

distances from the η^2_{OO}-Ni(CO_2) ($^3B_2$) structure and found a direct oxygen abstraction pathway to the NiO ($^3\Pi$) + CO asymptote. However, the located transition state (TS″ (^{3}A′), lying 59.9 kcal/mol above Ni (s^1d^9) + CO_2)) connects the Ni (s^1d^9) + CO_2 reactants directly with NiO ($^3\Pi$) + CO on the ^{3}A′ surface, as shown by our IRC calculations. All our further attempts to find a reaction channel between the η^2_{OO}-Ni(CO_2) structures and NiO + CO, or between η^2_{OO}-Ni(CO_2) and the ONiCO intermediates, failed in that we were not able to locate additional stationary points that could be relevant to these pathways (transition state optimizations converged either to TS′ (^{3}A′) or TS″ (^{3}A′)). We also tried to locate a direct oxygen abstraction on the ^{3}A″ surface. However, the located transition structure corresponds to a second-order saddle point. Its structure is similar to that on the ^{3}A′ surface, the second imaginary frequency corresponds to an out-of-plane motion. Transition structure optimization, starting from a slightly distorted geometry (C_1 symmetry) converged to the insertion transition (TS ^{3}A″), leading to the conclusion that the insertion−elimination route is the most favorable channel for the titled reaction.

(c) Overall Energetics and Relevance to Experiment. The energy diagram depicted in Figure 5 summarizes the CCSD-(T)/6-311+G(3df)′ energetics for the entire reaction. The diagram reveals that the only low-energy pathway for the Ni (s^1d^9) + CO_2 → NiO ($^3\Sigma^-$) + CO reaction is represented by the insertion route on the ^{3}A″ energy surface. The activation energy of this process is 34.5 kcal/mol, which is comparable to the endothermicity of the full reaction. Although the ONiCO (^{3}A″) intermediate formed along this route lies 15 kcal/mol above the reactants, this species is kinetically fairly stable

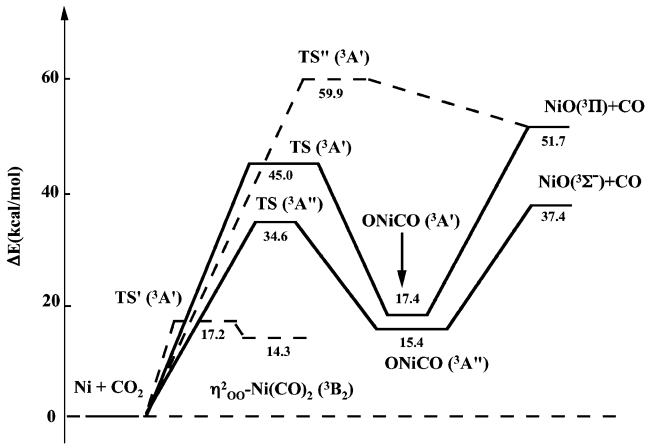

Figure 5. Energy diagram of the Ni + CO_2 → NiO + CO reaction derived from ZPE-corrected CCSD(T)/6-311+G(3df)′//B3LYP/6-311+G(3df)′ relative energies.

TABLE 3: Calculated B3LYP/6-311+G(3df)′ Vibrational Frequencies (cm^{-1}) and IR Intensities (km/mol in Parentheses) for ONiCO

mode character	ONiCO (^{3}A″)	ONiCO (^{3}A′)	exp[a]
CO stretching (a′)	2170 (906)	2165 (884)	2086.6, 2072.7
NiO stretching (a′)	743 (7)	611 (1)	
NiC stretching (a′)	408 (46)	421 (38)	
ip[b] OCNi bending (a′)	372 (3)	395 (0)	
oop[b] OCNi bending (a″)	339 (0)	351 (36)	
ONiC bending (a′)	100 (14)	92 (17)	

[a] From ref 23. These two absorption bands have been assigned to the same species in two different sites in argon matrix. [b] ip = in plane, oop = out of plane.

because its dissociation requires an energy of at least 20 kcal/mol. The metal insertion can also take place on the ^{3}A′ surface via an intermediate (ONiCO (^{3}A′)), being very close in energy to the ONiCO (^{3}A″) species; however, this route correlates with an excited state ($^3\Pi$) of NiO, which implies that the dissociation process is even less favored as compared to the ONiCO (^{3}A″) complex. In principle, the NiO ($^3\Pi$) molecule can also be produced via a direct oxygen abstraction reaction provided that a sufficient amount of input energy is available for the reactants, but the barrier along this route (TS″ (^{3}A′)) is higher by about 15 kcal/mol.

Finally, we wish to relate our results to the experimental evidence from matrix isolation studies.[19,23] As noted in the Introduction, the new product formed in the reactions of laser ablated Ni atoms with CO_2 was identified as the ONiCO insertion complex.[23] Our calculations predict this species to be the only feasible reaction intermediate for the title reaction corresponding to a well-defined minimum on both ^{3}A″ and ^{3}A′ surfaces, which is consistent with the above observation. Considering the excess kinetic energy of the laser-ablated metal atoms, both insertion channels might be accessible in the reaction (the participation of the Ni excited state cannot be ruled out). Not only the relative stabilities of the ONiCO (^{3}A″) and ONiCO (^{3}A′) species are similar, but also their predicted IR spectra show a close resemblance (Table 3). For instance, the CO stretching frequencies of these species differ only by a few wavenumbers. The sole vibrational mode that might serve as a reference to differentiate between the two species is the NiO stretching vibration, but this mode is not expected to give detectable bands, as judged from the calculated IR intensities. However, the observed bands decreased on photolysis, leading to the formation of NiO ($^3\Sigma^-$) and CO.[23] These bands then increased on annealing, indicating that the ONiCO species can

also be produced by a recombination of NiO ($^3\Sigma^-$) and CO. The observed species is thus the $^3A''$ insertion product because, as we have shown, there is no barrier for the NiO ($^3\Sigma^-$) + CO → ONiCO ($^3A''$) reaction. We have not analyzed the singlet state surfaces in the present study, but we mention that the relative stability of the η^2_{CO}-Ni(CO_2) ($^1A'$) complex is predicted to be −7.8 kcal/mol at the CCSD(T)/6-311+G(3df)′ level. The observation that thermally generated Ni atoms are unreactive with CO_2 in an argon matrix[19] suggest that the intersystem crossing between the triplet and singlet states is probably high enough and it is accessible by thermally produced metal atoms only with low probability. Further theoretical work is required to confirm this argument.

4. Conclusions

Combined B3LYP/CCSD(T) calculations were performed to describe the reaction of CO_2 with a Ni atom. We obtained that the lowest energy path proceeds through the $^3A''$ ONiCO intermediate and yields the $^3\Sigma^-$ NiO and CO. This reaction is initiated with 34.6 kcal/mol activation energy. We identified a similar reaction path on the $^3A'$ surface, but we found that all the stationary points are considerably higher in energy than those on the $^3A''$ surface. The metal insertion reaction is initiated by an electron transfer from the Ni atom to the CO_2 molecule and then the insertion and oxygen-abstraction steps take place in a concerted fashion along with the charge-transfer processes. We would like to point out that the insertion reaction is not preceded by η^2_{CO} complex formation as in the cases of Sc,[43] Ti,[41] and V[40] + CO_2 reactions. Also, in contrast to either Sc,[43] Ti,[35,41] or V,[40] the insertion of Ni to CO_2 is an endothermic reaction by 15.4 kcal/mol with respect to Ni (s^1d^9) + CO_2.

Acknowledgment. J.M., Y.H., and I.P. thank CNRS and HAS for allowing collaborative work through visits to Bordeaux and Budapest (Balaton 2000 and 2001/00851QL). J.M. acknowledges the allocation of computer time (IDRIS project No 11441). Y.H. acknowledges computational facilities provided with the M3PEC (DRIMM) at the University Bordeaux 1. Financial support from the Hungarian Research Foundation (OTKA T 034547 and T 037345) and from INTAS program (project 00-00911) are also acknowledged.

References and Notes

(1) Palmer, D. A.; van Eldik, R. *Chem. Rev.* **1983**, *83*, 651.
(2) Behr, A. Angew. *Chem. Int. Ed. Engl.* **1988**, *27*, 661.
(3) Braunstein, P.; Matt, D.; Nobel, D. *Chem. Rev.* **1988**, *88*, 747.
(4) Aresta, M., Schloss, J. V., Eds. *Enzymatic and Model Carboxylation and Reduction Reactions for Carbon Dioxide Utilization*; NATO ASI Ser. C No. 314; Kluwer: Dordrecht, The Netherlands, 1990.
(5) Leitner, W. *Coord. Chem. Rev.* **1996**, *153*, 257.
(6) Gibson, D. H. *Chem. Rev.* **1996**, *96*, 2063.
(7) Yin, X.; Moss, J. R. *Coord. Chem. Rev.* **1999**, *181*, 27.
(8) Song, C., Gaffney, A. M., Fujimoto, K., Eds. *CO_2 Conversion and Utilization*; ACS Symposium Series No. 809; American Chemical Society; Washington, DC, 2002.
(9) Arakawa, H.; Aresta, M.; Armor, J. N.; Barteau, M. A.; Beckman, E. J.; Bell, A. T.; Bercaw, J. E.; Creutz, C.; Dinjus, E.; Dixon, D. A.; Domen, K.; Dubois, D. L.; Eckert, J.; Fujita, E.; Gibson, D. H.; Goddard, W. A.; Goodman, D. W.; Keller, J.; Kubas, G. J.; Kung, H. H.; Lyons, J. E.; Manzer, L. E.; Marks, T. J.; Morokuma, K.; Nicholas, K. M.; Periana, R.; Que, L.; Rostrup-Nielson, J.; Sachtler, W. M. H.; Schmidt, L. D.; Sen, A.; Somorjai, G. A.; Stair, P. C.; Stults, B. R.; Tumas, W. *Chem. Rev.* **2001**, *101*, 953.
(10) McClean, R. E.; Pasternack, L. *J. Phys. Chem.* **1992**, *96*, 9828.
(11) Campbell, M. L.; McClean, R. E. *J. Phys. Chem.* **1993**, *97*, 7942.
(12) McClean, R. E.; Campbell, M. L.; Goodwin, R. H. *J. Phys. Chem.* **1996**, *100*, 7502.
(13) McClean, R. E.; Campbell, M. L.; Kolsch, E. J. *J. Phys. Chem. A* **1997**, *101*, 3348.
(14) Campbell, M. L.; Hooper, K. L.; Kolsch, E. J. *Chem. Phys. Lett.* **1997**, *274*, 7.
(15) Campbell, M. L.; Hooper, K. L. *J. Chem. Soc., Faraday. Trans.* **1997**, *93*, 2139.
(16) Campbell, M. L. *Chem. Phys. Lett.* **1998**, *294*, 339.
(17) Campbell, M. L. *J. Chem. Soc., Faraday. Trans.* **1998**, *934*, 1687.
(18) Campbell, M. L. *Phys. Chem. Chem. Phys.* **1999**, *1*, 3731.
(19) Mascetti, J.; Tranquille, M. *J. Phys. Chem.* **1988**, *92*, 2177.
(20) Chertihin, G. V.; Andrews, L. *J. Am. Chem. Soc.* **1995**, *117*, 1595.
(21) Souter, P. F.; Andrews, L. *J. Am. Chem. Soc.* **1997**, *119*, 7350.
(22) Zhou, M.; Andrews, L. *J. Am. Chem. Soc.* **1998**, *120*, 13230.
(23) Zhou, M.; Liang, B.; Andrews, L. *J. Phys. Chem. A* **1999**, *103*, 2013.
(24) Zhou, M.; Andrews, L. *J. Phys. Chem. A* **1999**, *103*, 2066.
(25) Wang, X.; Chen, M.; Zhang, L.; Qin, Q. *J. Phys. Chem. A* **2000**, *104*, 758.
(26) Chen, M.; Wang, X.; Zhang, L.; Qin, Q. *J. Phys. Chem. A* **2000**, *104*, 7010.
(27) Liang, B.; Andrews, L. *J. Phys. Chem. A* **2002**, *106*, 595.
(28) Caballol, R.; Marcos, E. S.; Barthelat, J. *J. Phys. Chem.* **1987**, *91*, 1328.
(29) Jeung, G. H. *Mol. Phys.* **1988**, *65*, 669.
(30) Jeung, G. H. *Mol. Phys.* **1989**, *67*, 747.
(31) Jeung, G. H. *Chem. Phys. Lett.* **1995**, *232*, 319.
(32) Sodupe, M.; Branchadell, V.; Oliva, A. *J. Phys. Chem.* **1995**, *99*, 8567.
(33) Rodriguez-Santiago, L.; Sodupe, M.; Branchadell, V. *J. Chem. Phys.* **1996**, *105*, 9966.
(34) Sodupe, M.; Branchadell, V.; Oliva, A. *J. Mol. Sruct. (THEOCHEM)* **1996**, *371*, 79.
(35) Pápai, I.; Mascetti, J.; Fournier R. *J. Phys. Chem. A* **1997**, *101*, 4465.
(36) Galan, F.; Fouassier, M.; Tranquille, M.; Mascetti, J.; Pápai, I. *J. Phys. Chem. A* **1997**, *101*, 2626.
(37) Mascetti, J.; Galan, F.; Pápai, I. *J. Coord. Chem. Rev.* **1999**, *190−192*, 557.
(38) Mele, F.; Russo, N.; Toscano, M.; Illas, F. In *New Trends in Quantum Systems in Chemistry and Physics*; Maruani, J., Ed.; Kluwer: Dordrecht, The Netherlands, 2000; Vol. 2.
(39) Mebel, A. M.; Hwang, D. *J. Phys. Chem. A* **2000**, *104*, 11622.
(40) Pápai, I.; Hannachi, Y.; Gwizdala, S.; Mascetti, J. *J. Phys. Chem. A* **2002**, *106*, 4181.
(41) Mebel, A. M.; Hwang, D. Y. *J. Chem. Phys.* **2002**, *116*, 5633.
(42) Hwang, D. Y.; Mebel, A. M. *Chem. Phys. Lett.* **2002**, *357*, 51.
(43) Pápai, I.; Schubert, G.; Hannachi, Y.; Mascetti, J. *J. Phys. Chem. A* **2002**, *106*, 9551.
(44) We assume a coplanar arrangement (C_s symmetry) of the interacting fragments all along the Ni + CO_2 → NiO + CO reaction.
(45) Becke, A. D. *J. Chem. Phys.* **1993**, *98*, 5648.
(46) Lee, C.; Yang, W.; Parr, R. G. *Phys. Rev. B* **1988**, *37*, 785.
(47) Stephens, P. J.; Devlin, F. J.; Chabalowski, C. F.; Frisch, M. J. *J. Phys. Chem.* **1994**, *98*, 11623.
(48) Schäfer, A.; Horn, H.; Ahlrichs, R. J. *Chem. Phys.* **1992**, *97*, 2571.
(49) Wachters, A. J. H. *J. Chem. Phys.* **1970**, *52*, 1033.
(50) Hay, P. J. *J. Phys. Chem.* **1977**, *66*, 43.
(51) Krishnan, R.; Binkley, J. S.; Seeger, R.; Pople, J. A. *J. Chem. Phys.* **1980**, *72*, 650. Frisch, M. J.; Pople, J. A.; Binkley, J. S. *J. Chem. Phys.* **1984**, *80*, 3265.
(52) Gonzalez, C.; Schlegel, H. B. *J. Chem. Phys.* **1989**, *90*, 2154.
(53) Calculations with the standard 6-311+G(3df) basis set led to unphysical symmetry breaking of the molecular orbitals, which was not observed when the Ni g functions were omitted from the basis set.
(54) Purvis, G. D.; Bartlett, R. J. *J. Chem. Phys.* **1982**, *76*, 1910.
(55) Pople, J. A., Head-Gordon, M.; Raghavachari, K. *J. Chem. Phys.* **1987**, *87*, 5968.
(56) Moore, S. E. *Atomic Energy Levels*; NSRDS: Washington, DC, 1971.
(57) Reed, A. E.; Curtiss, L. A.; Weinhold, F. *Chem. Rev.* **1988**, *88*, 899.
(58) Frisch, M. J.; Trucks, G. W.; Schlegel, H. B.; Scuseria, G. E.; Robb, M. A.; Cheeseman, J. R.; Zakrzewski, V. G.; Montgomery, J. A., Jr.; Stratmann, R. E.; Burant, J. C.; Dapprich, S.; Millam, J. M.; Daniels, A. D.; Kudin, K. N.; Strain, M. C.; Farkas, O.; Tomasi, J.; Barone, V.; Cossi, M.; Cammi, R.; Mennucci, B.; Pomelli, C.; Adamo, C.; Clifford, S.; Ochterski, J.; Petersson, G. A.; Ayala, P. Y.; Cui, Q.; Morokuma, K.; Malick, D. K.; Rabuck, A. D.; Raghavachari, K.; Foresman, J. B.; Cioslowski, J.; Ortiz, J. V.; Stefanov, B. B.; Liu, G.; Liashenko, A.; Piskorz, P.; Komaromi, I.; Gomperts, R.; Martin, R. L.; Fox, D. J.; Keith, T.; Al-Laham, M. A.; Peng, C. Y.; Nanayakkara, A.; Gonzalez, C.; Challacombe, M.; Gill, P. M. W.; Johnson, B. G.; Chen, W.; Wong, M. W.; Andres, J. L.; Head-Gordon, M.; Replogle, E. S.; Pople, J. A. *Gaussian98*, revision A.11.3; Gaussian, Inc.: Pittsburgh, PA, 1998.

(59) Structural parameters obtained at the B3LYP/6-311+G(2d)′ level are very similar to those of B3LYP/6-311+G(3df)′ data: optimized bond lengths and angles differ only by at most 0.01 Å and 0.7°, respectively.

(60) Watson, L. R.; Thiem, T. L.; Dressler, R. A.; Salter, R. H.; Murad, E. *J. Phys. Chem.* **1993**, *97*, 5577.

(61) Chase, M. W., Jr.; Davies, C. A.; Downey, J. R., Jr.; Frurip, D. J.; McDonald, R. A.; Syverud, A. N. *JANAF Tables*, 3rd ed.; J. Phys. Chem. Ref. Data; American Chemical Society: Washington, DC, 1985; Vol. 14, Suppl. 1.

(62) Ram, R. S.; Bernath, P. F. *J. Mol Spectrosc.* **1992**, *155*, 315.

(63) Becke, A. D. *Phys. Rev. A* **1988**, *38*, 3098.

(64) (a) Perdew, J. P., *Phys. Rev. B* **1986**, *33*, 8822. (b) Perdew, J. P. *Phys. Rev. B* **1986**, *34*, 7406.

(65) Hammond, G. S. *J. Am. Chem. Soc.* **1955**, *77*, 334.

(66) Stirling, A. *J. Am. Chem. Soc.* **2002**, *124*, 4058.

(67) Herzberg, G. *Molecular Spectra and Molecular Structure III. Electronic Spectra and Electronic Structure of Polyatomic Molecules*; Van Nostrand Reinhold: New York, 1966.

(68) Huber, K. P.; Herzberg, G. *Constants of Diatomic Molecules*; Van Nostrand Reinhold: New York 1979.

(69) Namiki, K.; Saito, S. *Chem. Phys. Lett.* **1996**, *252*, 343.